

Degeneracy and kink scattering in a two coupled scalar field model in (1, 1) dimensions

Fabiano C. Simas^{1,2}, K. Z. Nobrega³, D. Bazeia⁴, Adalto R. Gomes^{1,5*}

¹ *Programa de Pós-Graduação em Física,*

Universidade Federal do Maranhão (UFMA),

Campus Universitário do Bacanga, 65085-580, São Luís, Maranhão, Brazil

² *Centro de Ciências Agrárias e Ambientais-CCAA,*

Universidade Federal do Maranhão (UFMA),

65500-000, Chapadinha, Maranhão, Brazil

³ *Departamento de Engenharia Teleinformática,*

Universidade Federal do Ceará (UFC),

60455-640, Fortaleza, Ceará, Brazil

⁴ *Departamento de Física, Universidade Federal da Paraíba,*

58051-970, João Pessoa, PB, Brazil

⁵ *Departamento de Física, Universidade Federal do Maranhão (UFMA),*

Campus Universitário do Bacanga, 65085-580, São Luís, Maranhão, Brazil.

Abstract

In this paper we analyze the scattering process in a two-field model in $(1+1)$ -dimensions, with the special property to have several topological solutions: i) one with higher rest mass, characterized by a nested defect (lump inside a kink), and ii) four others having lower rest mass, degenerated, and characterized by a kink inside kink. We investigate kink-antikink symmetric scattering, where the kink and antikink have higher rest mass and the same initial velocity modulus v . The output of scattering presents a wide range of behaviors, such as annihilation of the kink-antikink pair, the emission of radiation jets, the generation of oscillating pulses and the change of the topological sector. We show that the changing of the topological sector is favored, and only two of the four sectors are possible as outcomes. Moreover, despite the degeneracy in energy, the distribution of the final states is asymmetric in the phase space, being an effect of the presence of vibrational states. This is likely a general effect, present in other two-field models with phenomenological interest.

*Electronic address: fc.simas@ufma.br, kznobrega@ufc.br, bazeia@fisica.ufpb.br, argomes.ufma@gmail.com

I. INTRODUCTION

Solitary waves are characterized by the very special property of free propagation without dispersion [1–3]. Solitary waves of special interest are topological defects in nonlinear field theories, where stability of a localized energy density is related to a conserved topological current. The simplest topological defect is the (1, 1) dimensional kink (and the corresponding antikink), which appears in the model with degenerate minima potentials. The kink embedded in higher dimensions generate domain walls. Kinks and domain walls have been explored theoretically or observed in systems of variable complexity and energy scales, such as condensed matter physics (for instance ferromagnetics materials [4], superfluid ^3He [5, 6], twisted nematic liquid crystals [7], superconductors [8, 9]), nuclear physics and QCD [10–12], cosmology [3, 13, 14], optics [15–17] and biochemistry [18].

In integrable models, the kink-antikink scattering is simpler in comparison to the observed for nonintegrable models. The sine-Gordon model constitutes an example of an integrable model, with the defects gaining at most a phase shift after scattering [19]. An essential aspect to be investigated is how the lack of integrability affects the kink collision process. As an example, the kink-antikink scattering in the nonintegrable ϕ^4 model exhibits a rich pattern of scattering [20–27]. There is a critical initial velocity v_c that characterizes the scattering scenario. For $v < v_c$, the kink-antikink pair forms a composed state named bion that radiate continuously. For larger initial velocities, we have inelastic scattering, with the pair colliding once and escaping to infinity. In addition, for $v \lesssim v_c$ it can occur resonant two-bounce collision [22], were the kink-antikink ($K\bar{K}$) pair escapes to infinity after two collisions. This phenomenon can be explained by the energy exchange mechanism between zero and vibrational modes [22]. Kink scattering was also investigated in other single scalar field nonintegrable models [28–41], kink dynamics with impurities [42–49], scattering with a boundary [50, 51] and multi-kink collision [52, 53]. The role of quasi-normal modes in the scattering process was investigated in the Refs. [54, 55], and spectral walls in the Refs. [56, 57].

The experimental evidence of kink motion in condensed matter systems is an active area of research, with potentially important applications. For instance, kink motion in single walled carbon nanotubes are connected with superplasticity, and could strengthen and toughen ceramics and other nanocomposites at high temperatures. [58]. The multiplication,

dissociation, and screw motion of kinks in nanotubes was reported in the Ref. [59]. There is experimental evidence that the kink motion is a universal plastic deformation mode in all nanotubes when they were under external stress and high temperatures. Some studies of numerical investigation can also be cited. A microscopic mechanism for kink motion in nanotubes considered the removal of the carbon atom with the highest energy within a single framework of molecular dynamics [60]. In perpendicular magnetized thin films, the presence of the Dzyaloshinskii-Moriya interaction opens up the possibility, through electric field controlled anisotropies, of efficient control of domain wall motion with electric fields, with applications in spintronic [61]. Kink scattering for the graphene superlattice equation showed bounce windows with fractal structure [62].

As described above, the kink-antikink scattering in nonintegrable single-field models has a complex structure. Then, in systems with two scalar fields, we can expect a more intricate behavior. Models with two or more scalar fields can be used to describe kinks in condensed matter, that describe for instance rotational and torsional degrees of freedom of the DNA molecule [63] and proton conductivity in Langmuir films [64]. Kink-antikink dynamics in models with two scalar fields was investigated in the Refs. [65–70]. Of particular interest in this paper is the model of two coupled scalar fields ϕ, χ in $(1, 1)$ dimensions introduced in the Ref. [71]. The model has a coupling parameter r such that in a topological sector there are explicit kink (K_{21}) and antikink (\bar{K}_{21}) solutions for $0 < r < 1/2$ in a form of nested defects, where the field ϕ has a kink (antikink) profile whereas the χ field has a lump one. There are four other topological sectors with kinks degenerated with a lower energy, where both fields have a kink (or antikink) profile. The formed defects have internal structure similar to the obtained in the Bloch wall scenario obtained in the Ginzburg-Landau equation describing magnetic systems [72]. Also this model was considered in a scenario with domain wall with internal structure embedded in other defect of higher dimensions [73].

In the next section we present the model. In the section III we present the numerical analysis of kink-antikink scattering, showing how the initial higher energy solution can be traded by other solutions degenerate in energy, with some interesting effects. We conclude in the section IV.

II. THE MODEL

We consider a two-coupled scalar field model with (1,1)-dimensional governed by the action

$$S = \int dt dx \left[\frac{1}{2} \partial_\mu \phi \partial^\mu \phi + \frac{1}{2} \partial_\mu \chi \partial^\mu \chi - V(\phi, \chi) \right], \quad (1)$$

where the potential $V = V(\phi, \chi)$ is a function of partial derivatives of a smooth function $W(\phi, \chi)$ as

$$V(\phi, \chi) = \frac{1}{2} W_\phi^2 + \frac{1}{2} W_\chi^2. \quad (2)$$

The energy density of static solutions are given by

$$\mathcal{E}(x) = \pm \frac{dW}{dx} + \frac{1}{2} \left(\frac{d\phi}{dx} \mp W_\phi \right)^2 + \frac{1}{2} \left(\frac{d\chi}{dx} \mp W_\chi \right)^2. \quad (3)$$

Then, solutions satisfying the first-order equations

$$\frac{d\phi}{dx} = \pm W_\phi, \quad \frac{d\chi}{dx} = \pm W_\chi, \quad (4)$$

are BPS solutions and minimize energy. The plus sign in the Eqs. (4) will result in kinks whereas the minus sign to antikinks. The energy of the solutions are given by $E_{BPS} = |W[\phi(+\infty), \chi(+\infty)] - W[\phi(-\infty), \chi(-\infty)]|$. In this work we consider the function [71]

$$W(\phi, \chi) = \phi - \frac{1}{3} \phi^3 - r \phi \chi^2, \quad (5)$$

with r a positive constant. This corresponds to the potential

$$V(\phi, \chi) = \frac{1}{2} (1 - \phi^2 - r \chi^2)^2 + 2r^2 \phi^2 \chi^2, \quad (6)$$

This potential has minima at $v_{1,2}(\pm 1, 0)$ and $v_{3,4}(0, \pm 1/\sqrt{r})$, and have five BPS sectors connecting the minima v_i and v_j with energy E_{ij} : one with energy $E_{12} = 4/3$ and four degenerate sectors with energy $E_{13} = E_{14} = E_{23} = E_{24} = 2/3$.

The equations of motion are given by

$$\frac{\partial^2 \phi}{\partial t^2} - \frac{\partial^2 \phi}{\partial x^2} + \frac{dV(\phi, \chi)}{d\phi} = 0, \quad (7)$$

$$\frac{\partial^2 \chi}{\partial t^2} - \frac{\partial^2 \chi}{\partial x^2} + \frac{dV(\phi, \chi)}{d\chi} = 0. \quad (8)$$

and the first-order equations for kinks are given by

$$\frac{d\phi}{dx} = 1 - \phi^2 - r\chi^2, \quad (9)$$

$$\frac{d\chi}{dx} = -2r\phi\chi. \quad (10)$$

These equations can be solved using the trial orbits method [74] or after finding an integrating factor [75], leading to the K_{21} -kink solutions connecting the minima $v_2(-1, 0)$ and $v_1(1, 0)$ for $0 < r < 1/2$, and given by

$$\phi_{21}(x, r) = \tanh(2rx), \quad (11)$$

$$\chi_{21}(x, r) = \sqrt{\frac{1}{r} - 2\text{sech}(2rx)}. \quad (12)$$

Similarly, \bar{K}_{21} -antikink solutions of Eqs. (4) with minus sign connecting the minima $v_2(1, 0)$ and $v_1(-1, 0)$ for $0 < r < 1/2$ are given by

$$\bar{\phi}_{21}(x, r) = -\phi_{21}(x, r) = -\tanh(2rx), \quad (13)$$

$$\bar{\chi}_{21}(x, r) = \chi_{21}(x, r) = \sqrt{\frac{1}{r} - 2\text{sech}(2rx)}. \quad (14)$$

The other degenerated solutions for the other topological sectors are i) The K_{31} -kink solution connecting the minima $v_3(0, 1/\sqrt{r})$ and $v_1(1, 0)$; The K_{41} -kink solution connecting the minima $v_4(0, -1/\sqrt{r})$ and $v_1(1, 0)$; iii) The K_{23} -kink solution connecting the minima $v_2(-1, 0)$ and $v_3(0, 1/\sqrt{r})$; iv) iii) The K_{24} -kink solution connecting the minima $v_2(-1, 0)$ and $v_4(0, -1/\sqrt{r})$. These solutions are degenerate in energy and orbits in the phase space (ϕ, χ) can be found using the integrating factor [74]. However, explicit x -dependence of them can be found only for very specific values of r .

Note also that in all degenerate solutions, both fields ϕ and χ interpolate between different

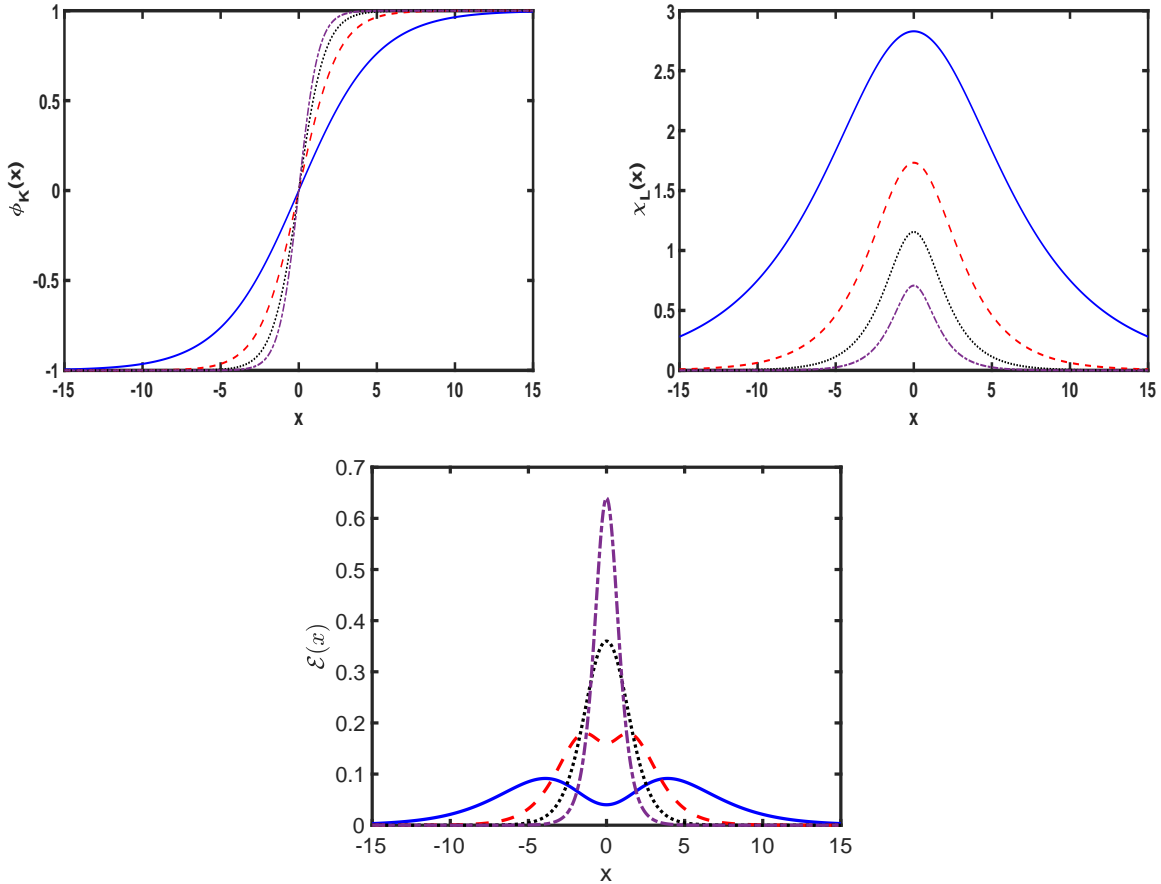


FIG. 1: The K_{21} -kink solution connecting the minima $v_2(-1, 0)$ and $v_1(1, 0)$, showing the components a) $\phi_{21}(x)$, b) $\chi_{21}(x)$ and (c) the energy density $\mathcal{E}(x)$. In the figures we fixed $r = 0.1$ (blue line), $r = 0.2$ (red dash), $r = 0.3$ (black dot) and $r = 0.4$ (purple dash-dot).

minima, whereas for the solution K_{21} , the field χ has a lump structure. This is depicted in the Figs. 1a and 1b. The energy density $\mathcal{E}(x)$ of this solution is depicted in the Figs. 1c for several values of r . Note from the figure that for $0.3 < r < 0.5$ one has a peak centered at $x = 0$. For $r = 0.3$ there is a plateau at $x = 0$. For $0 < r < 0.3$ there is the appearance of two peaks in the energy density, showing that the defect has an internal structure. That is, we have a nested defect, where the field χ is in the core of the defect and contributes to enrich its energy density. Domain walls with internal structure were observed in ferromagnets [78]. A similar solution was obtained for an extension of this model with extra dimensions and gravity in the Ref. [?]. Since this solution is more complex and more energetic, with known analytical solution for the range $0 < r < 1/2$, in the following section we will consider the kink-antikink scattering with solutions K_{21} and \bar{K}_{21} .

III. NUMERICAL RESULTS

In this section we describe the numerical results concerning the scattering process of the K_{21} -kink. For this process, we solved the two equations of motion (Eqs. (7) and (8)) with a 4th order finite-difference method with a spatial step $\delta x = 0.05$. We fixed $x = \pm x_0 = \pm 20$ for the initial symmetric position of the pair. For the time dependence we used 6th order symplectic integrator method, with a time step $\delta t = 0.02$. We used the following initial conditions for scattering

$$\phi(x, 0, x_0, v, r) = \phi_K(x + x_0, 0, v, r) - \phi_K(x - x_0, 0, -v, r) - 1 \quad (15)$$

$$\dot{\phi}(x, 0, x_0, v, r) = \dot{\phi}_K(x + x_0, 0, v, r) - \dot{\phi}_K(x - x_0, 0, -v, r), \quad (16)$$

and

$$\chi(x, 0, x_0, v, r) = \chi_L(x + x_0, 0, v, r) + \chi_L(x - x_0, 0, -v, r) \quad (17)$$

$$\dot{\chi}(x, 0, x_0, v, r) = \dot{\chi}_L(x + x_0, 0, v, r) - \dot{\chi}_L(x - x_0, 0, -v, r), \quad (18)$$

where $\phi_K(x, t, v, r) = \phi_{21}(\gamma(x - vt), r)$ and $\chi_L(x, t, v, r) = \chi_{21}(\gamma(x - vt), r)$ means a boost for the static solution with $\gamma = (1 - v^2)^{-1/2}$.

To better understand the scattering process of the K_{21} -kink, we will consider separately its components $\phi(x)$ and $\chi(x)$. The structure of our results of scattering process is presented in the Figs. 2a and 2b. There we observe the bidimensional (v, r) phase space, that corresponds the final state of scalar fields $\phi(x = 0, t_f)$ and $\chi(x = 0, t_f)$. We noticed in the figures the presence of intricate patterns. An important think to note is that the structure of the phase space is roughly the same in both figures. This indicate that the scalar fields ϕ and χ do not decouple after scattering, and we have still a defect with internal structure. From the the diagrams we can identify nine regions, labeled from A to I, and showed in the Fig. 2b. Now we will consider separately the characteristics of each region. Remember that we are considering collisions of the type $K_{21}\bar{K}_{21}$, where the solution K_{21} interpolates between the vacua $v_2(-1, 0)$ and $v_1(1, 0)$. In particular, the behavior for $x \rightarrow -\infty$ is fixed. This means that only two of the four topological sectors are possible as outputs.

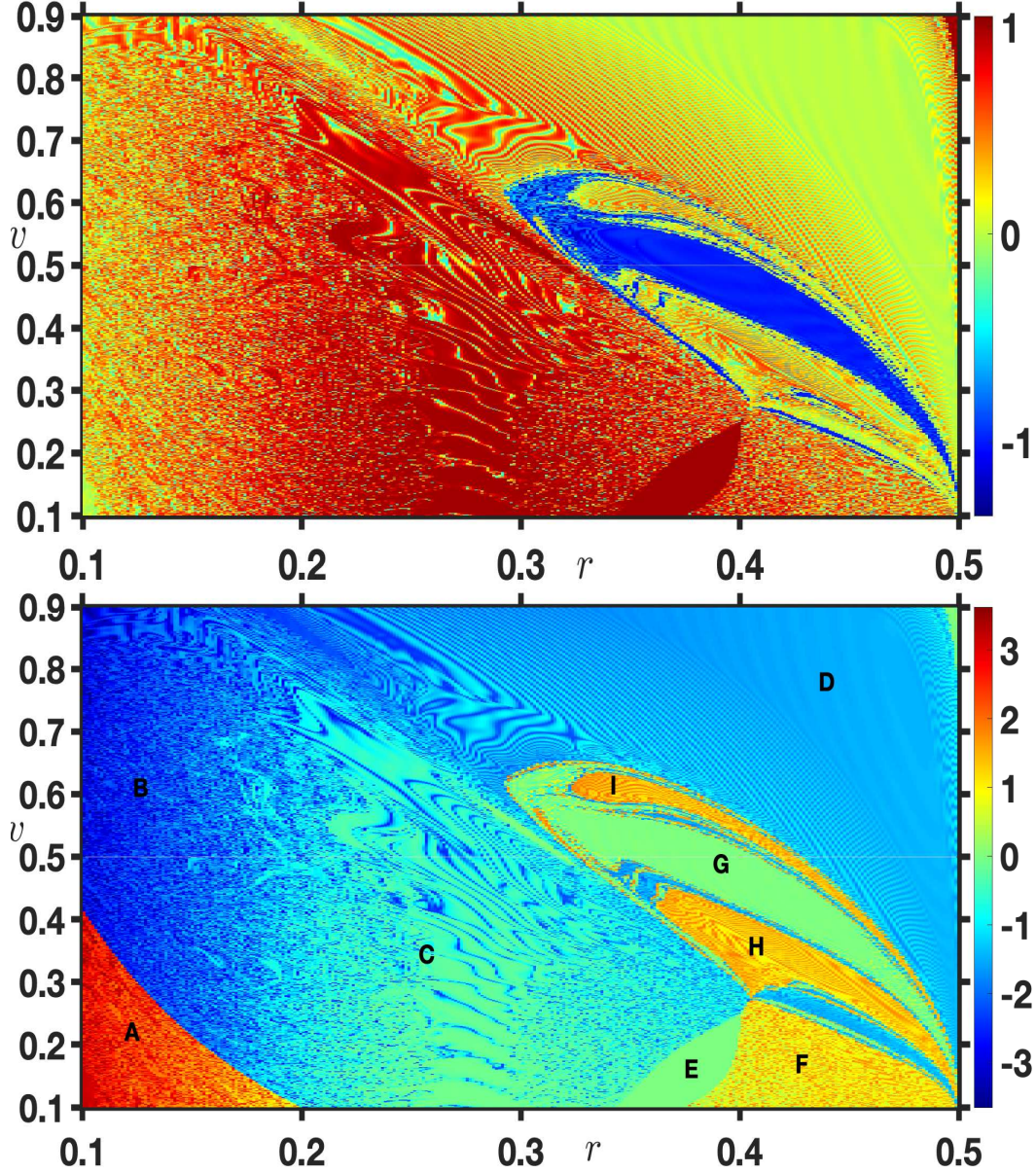


FIG. 2: Output of the $K_{21}\bar{K}_{21}$ collision process: a) (top) Final state of the scalar field $\phi_K(x = 0, t_f)$, b) (bottom) Final state of the scalar field $\chi_K(x = 0, t_f)$. Here one can also see the different regions labeled from A to I.

- region A - This region has collisions represented in the Figs. 3. For $x < 0$ note that the ϕ -component changes from $-1 \rightarrow 1$ to $-1 \rightarrow 0$, whereas the χ -component changes to $0 \rightarrow 0$ to $0 \rightarrow 3$, meaning that the K_{21} -kink changes to K_{23} after scattering. For $x > 0$ one can make a similar reasoning: the ϕ -component changes from $1 \rightarrow -1$ to $0 \rightarrow -1$, and the χ -component from $0 \rightarrow 0$ to $3 \rightarrow 0$, meaning that the \bar{K}_{21} -antikink changes to \bar{K}_{23} after scattering. Then, the collision can be characterized by

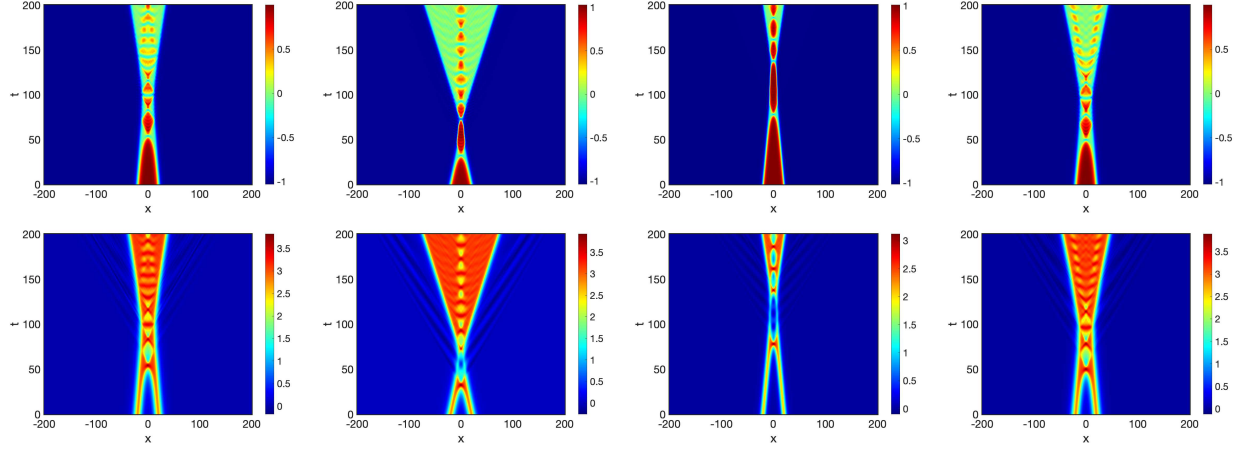


FIG. 3: Region A - ϕ -component (top) and χ -component (botton) for (a) $v = 0.14$ with $r = 0.104$ (b) $v = 0.37$ with $r = 0.10$, (c) $v = 0.158$ with $r = 0.162$ and (d) $v = 0.15$ with $r = 0.10$.

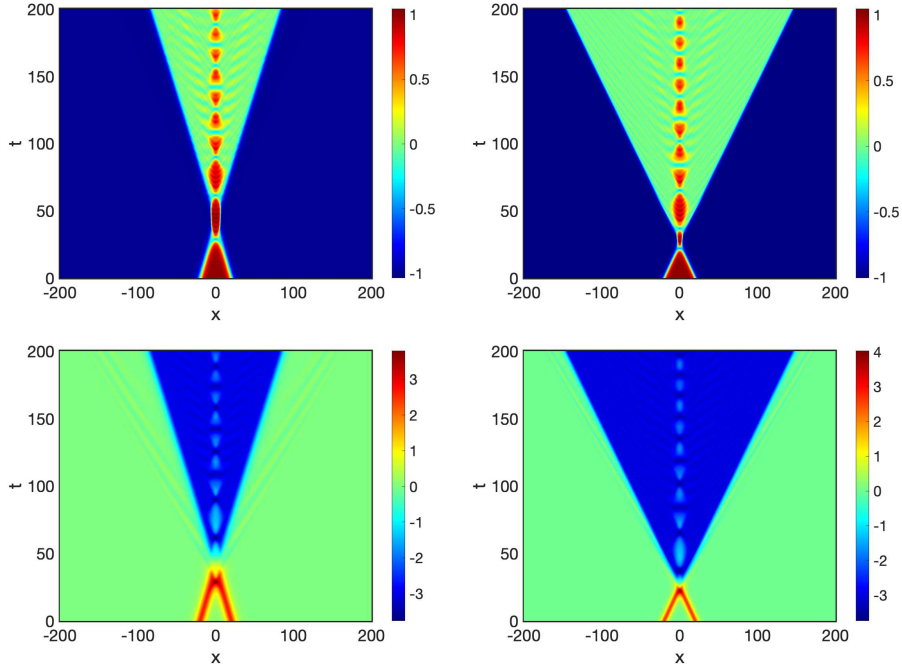


FIG. 4: Region B - ϕ -component (top) and χ -component (bottom) for (a) $v = 0.50$ with $r = 0.11$ and (b) $v = 0.80$ with $r = 0.11$

$K_{21} + \bar{K}_{21} \rightarrow K_{23} + \bar{K}_{23}$ and the production of a stationary oscillation around $x = 0$. We noted that the emission of radiation is more evidently produced by the χ -component.

- region B - This region has collisions represented in the Figs. 4. For $x < 0$ note that the ϕ -component changes from $-1 \rightarrow 1$ to $-1 \rightarrow 0$, whereas the χ -component changes to $0 \rightarrow 0$ to $0 \rightarrow -3$, meaning that the K_{21} -kink changes to K_{24} after scattering. For

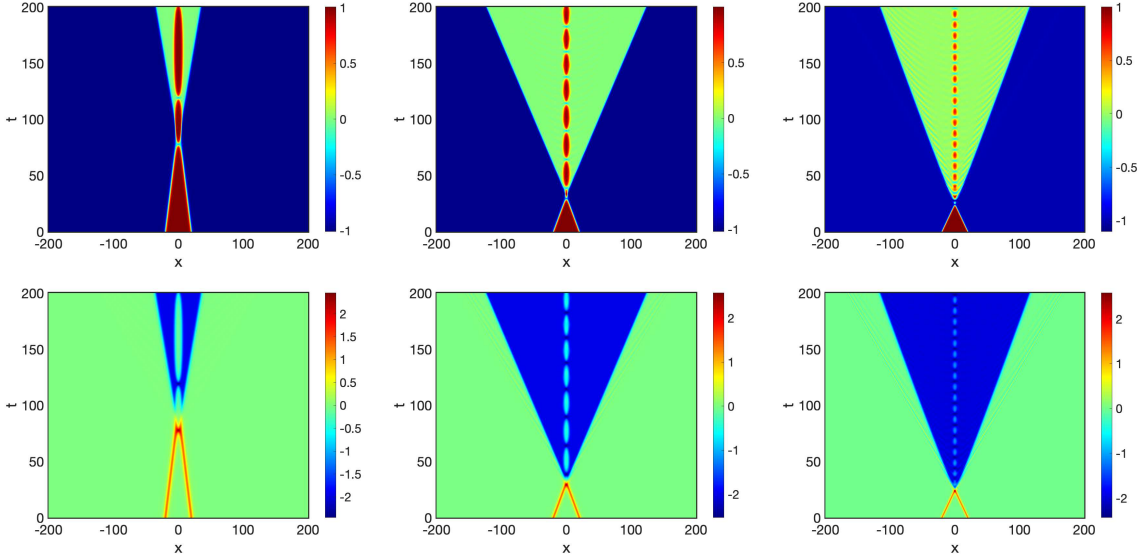


FIG. 5: Region C - ϕ -component (top) and χ -component (bottom) for (a) $v = 0.21$ with $r = 0.27$, (b) $v = 0.64$ with $r = 0.25$ and (c) $v = 0.82$ with $r = 0.255$.

$x > 0$ one can make a similar reasoning: the ϕ -component changes from $1 \rightarrow -1$ to $0 \rightarrow -1$, and the χ -component from $0 \rightarrow 0$ to $-3 \rightarrow 0$, meaning that the \bar{K}_{21} -antikink changes to \bar{K}_{24} after scattering. Then, the collision can be characterized by $K_{21} + \bar{K}_{21} \rightarrow K_{24} + \bar{K}_{24}$ and the production of a stationary oscillation around $x = 0$. We noted that the emission of radiation is more evidently produced by the χ -component.

- region C - This region has collisions represented by the Figs. 5. The results from this region are very similar from those in region B, since they are also characterized by $K_{21} + \bar{K}_{21} \rightarrow K_{24} + \bar{K}_{24}$. The difference is that the oscillations around $x = 0$, the scalar field ϕ span more time in the vacuum $\phi = 1$, and less around $\phi = 0$.
- region D - This region has collisions represented by the Figs. 6. The results from this region are very similar from those in region B, since they are also characterized by $K_{21} + \bar{K}_{21} \rightarrow K_{24} + \bar{K}_{24}$. The difference is that there is no significative oscillations around $x = 0$.
- region E - This region has collisions represented by the Figs. 7. We note the invariance in the fields around $x = 0$, except for the small interval of time where the collision occurs. However, the figure shows the emission of two symmetric thin $K_{24}\bar{K}_{24}$ pairs.
- region F - This region has collisions represented by the Figs. 8. This region is char-

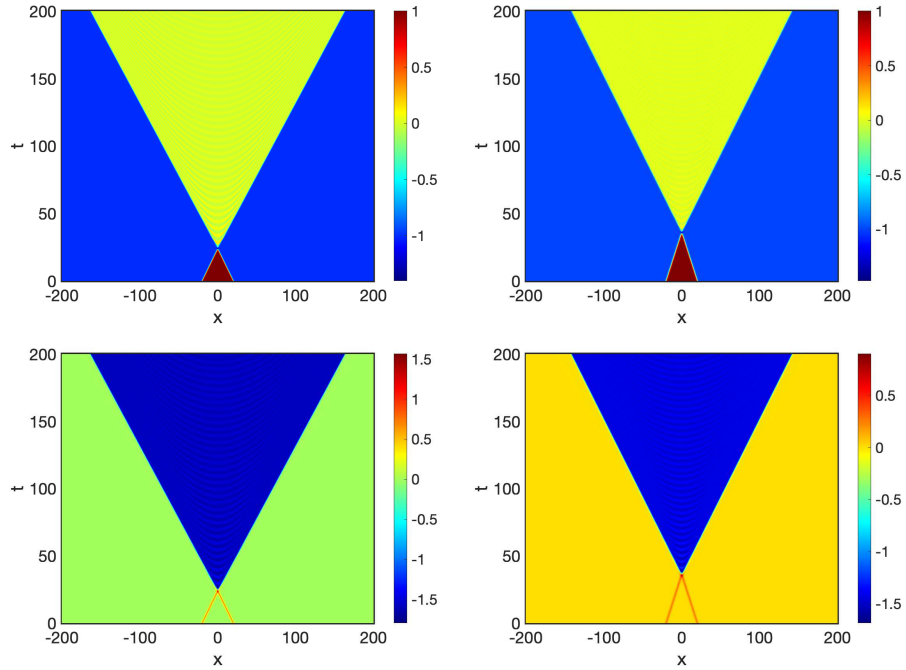


FIG. 6: Region D - ϕ -component (top) and χ -component (bottom) for (a) $v = 0.84$ with $r = 0.40$ and (b) $v = 0.555$ with $r = 0.483$.

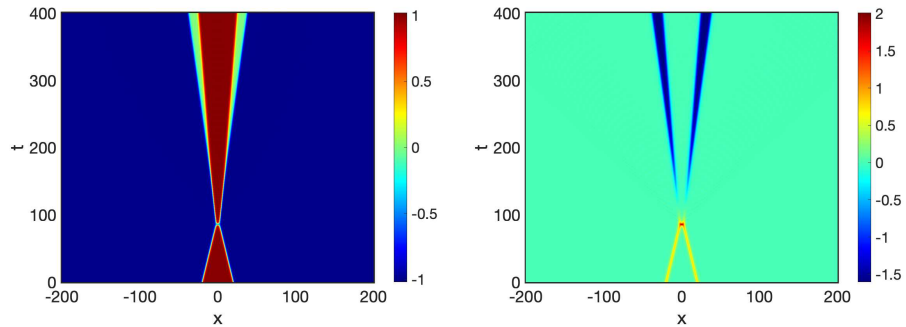


FIG. 7: Region E - ϕ -component (left) and χ -component (right) for $v = 0.208$ with $r = 0.392$.

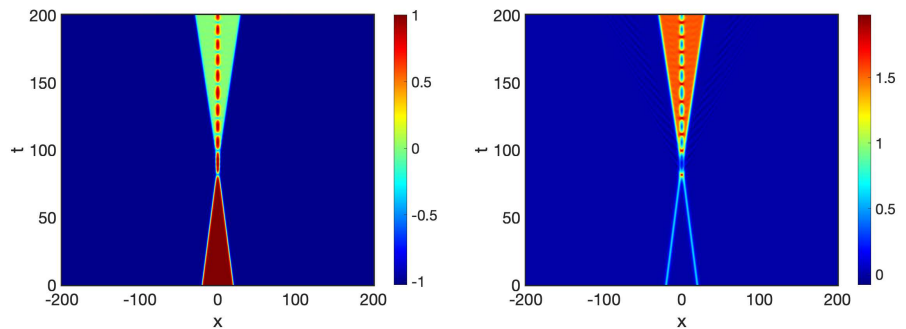


FIG. 8: Region F - ϕ -component (left) and χ -component (right) for $v = 0.223$ with $r = 0.42$.

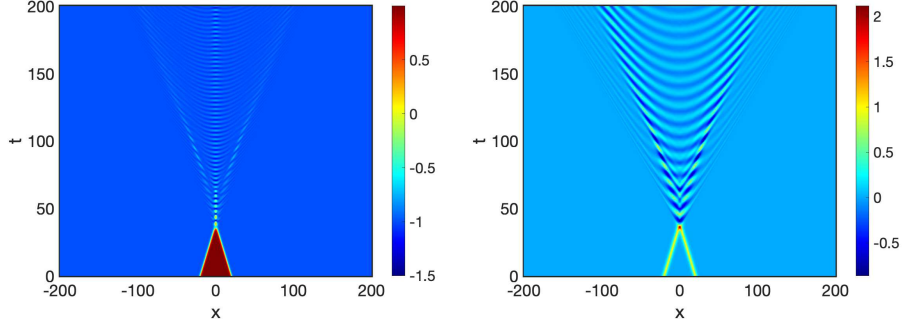


FIG. 9: Region G - ϕ -component (left) and χ -component (right) for $v = 0.524$ with $r = 0.336$.

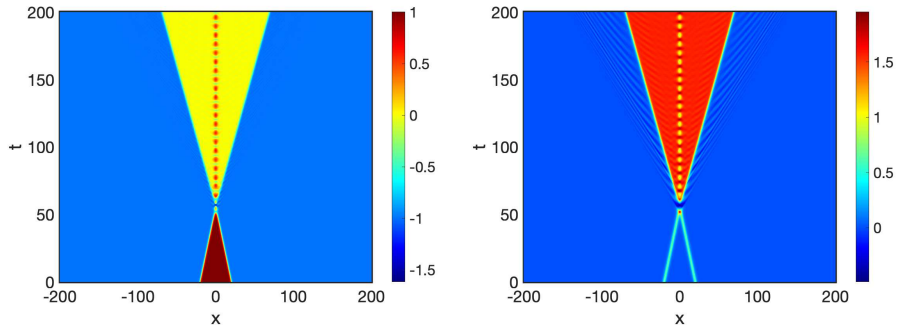


FIG. 10: Region H - ϕ -component (left) and χ -component (right) for (a) $v = 0.3618$ with $r = 0.4085$.

acterized by scattering of the type $K_{21} + \bar{K}_{21} \rightarrow K_{23} + \bar{K}_{23}$ and a central oscillations around $x = 0$. Note that, contrary to what observed in the region A, the oscillations are very localized, with no significant distortion.

- region G - This region has collisions represented by the Figs. 9. In this region the defects annihilate, with the fields restoring to the vacua $(\phi, \chi) = (-1, 0)$. The ϕ component produces two symmetric radiation jets and a localized oscillation around $x = 0$. The χ field produces delocalized radiation.
- region H - This region has collisions represented by the Figs. 10. The results are similar from those in the region F.
- region I - This region has collisions represented by the Figs. 11. The results are similar from those in the region F.

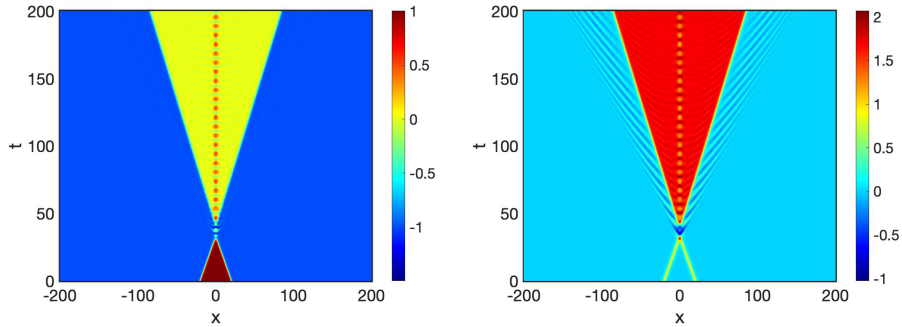


FIG. 11: Region I - ϕ -component (left) and χ -component (right) for $v = 0.609$ with $r = 0.346$.

IV. CONCLUSIONS

In this work we considered a two-scalar field model with kink solutions connecting five topological sectors, with four of them degenerate in energy. We considered kink-antikink scattering of the more energetic kink, K_{21} , from where an explicit x -dependence is known. We studied the effect of the coupling r and initial velocity v on the scattering. We noted that the phase diagram of the ϕ -component matches that of the χ -component. This shows that the scalar fields do not uncouple after the scattering, keeping the character of a nested defect. The structure of the phase diagram is complex, but it shows several regions where there the scattering is characterized by $K_{21} + \bar{K}_{21} \rightarrow K_{23} + \bar{K}_{23}$ or $K_{21} + \bar{K}_{21} \rightarrow K_{24} + \bar{K}_{24}$. There are differences in the regions concerned to the presence or absence of oscillations around $x = 0$ and their degree of dispersion. There is region where the collision results in complete annihilation of the pair, an another region that produces two thin $K_{24}\bar{K}_{24}$ pairs.

Despite the degeneracy in energy, the phase diagram is not symmetric concerning to the production of K_{23} and K_{24} kinks. This can be related to other aspects of these solutions, such as the presence of vibrational states from the linear perturbation analysis. However, for making a linear stability analysis, explicit solutions with dependence with x and r would be of interest. Unfortunately such solutions are not known for K_{23} and K_{24} , in the whole range of values of r which we consider in the present investigation. From the vacua structure of the model, one would expect that $K_{23} \rightarrow K_{24}$ after the transformation $(\phi, \chi) \rightarrow (\phi, -\chi)$, a symmetry which is not present in the phase diagram displayed in the Fig. 2. To better understand this issue, we note that the matrix potential of linear perturbations is not invariant

under this transformation. To see how this works explicitly, let us consider

$$\phi(x) = \phi_s(x) + \eta_n(x) \cos(\omega_n t), \quad (19)$$

$$\chi(x) = \chi_s(x) + \xi_n(x) \cos(\omega_n t). \quad (20)$$

Substituting these equations into the equations of motion, we get the matrix operator

$$\left(-\mathbf{1} \frac{d^2}{dx^2} + \mathbf{M} \right) \begin{pmatrix} \eta_n \\ \xi_n \end{pmatrix} = \omega_n^2 \begin{pmatrix} \eta_n \\ \xi_n \end{pmatrix}, \quad (21)$$

where the $\mathbf{1}$ is the 2×2 identity matrix and

$$\mathbf{M} = \begin{pmatrix} V_{\phi\phi} & V_{\phi\chi} \\ V_{\chi\phi} & V_{\chi\chi} \end{pmatrix} \quad (22)$$

is the matrix potential of perturbations. For the model considered we have $V_{\phi\phi} = 6\phi^2 + (4r^2 + 2r)\chi^2 - 2$, $V_{\chi\chi} = (4r^2 + 2r)\phi^2 + 6r^2\chi^2 - 2r$ and $V_{\phi\chi} = V_{\chi\phi} = (8r^2 + 4r)\phi\chi$. That is, the nondiagonal terms $V_{\phi\chi}$ and $V_{\chi\phi}$ of the matrix M are not invariant under the transformation $(\phi, \chi) \rightarrow (\phi, -\chi)$. Then, despite symmetric and degenerate, the solutions K_{23} and K_{24} are not symmetric under linear perturbations, resulting in the complex behavior described in this work.

We also noted the absence of the generation of K_{13} e K_{14} in the scattering. This is due to the values of the vacua: $(\phi, \chi) = (-1, 0)$ at $x \rightarrow -\infty$ and $(\phi, \chi) = (1, 0)$ at $x \rightarrow +\infty$. From the symmetry of the solutions, one expects to generate such kinks in the $\bar{K}_{21}K_{21}$ scattering. Indeed, the pattern of the $\bar{K}_{21}K_{21}$ scattering is the same observed for the $K_{21}\bar{K}_{21}$, with same output states after the transformation $K_{23} \rightarrow K_{13}$ and $K_{24} \rightarrow K_{14}$.

V. ACKNOWLEDGEMENTS

F.C.S. and A.R.G. thank FAPEMA - Fundação de Amparo à Pesquisa e ao Desenvolvimento do Maranhão through Grants PRONEM 01852/14, Universal 00920/19, 01191/16 and 01441/18. A.R.G. thanks CNPq (brazilian agency) through Grants 437923/2018-5 and 311501/2018-4 for financial support. This study was financed in part by the Coordenação

de Aperfeiçoamento de Pessoal de Nível Superior - Brasil (CAPES) - Finance Code 001. D.B. acknowledges CNPq (Grants No. 303469/2019-6 and No. 404913/2018-0) and Paraíba State Research Foundation (Grant 0015/2019) for financial support.

- [1] T. Dauxois and M. Peyrard, *Physics of solitons*, Cambridge University Press, Cambridge, U.K. (2006).
- [2] E.J. Weinberg, *Classical solutions in quantum field theory*, Cambridge Monographs on Mathematical Physics, Cambridge University Press, Cambridge, U.K. (2012).
- [3] T. Vachaspati, *Kinks and domain walls*, Cambridge Univ. Press, Cambridge, U.K. (2006).
- [4] Jona F, Shirane G. *Ferroelectric crystals*. New York: Dover; 1993. B.A. Strukov and A. Levanyuk, *Ferroelectric Phenomena in Crystals*, Berlin, Springer-Verlag.
- [5] Yasumasa Tsutsumi, Mass current at a domain wall in superfluid ^3He A-Phase, *Journ. Low Temp. Phys.*, 175, 51 (2014).
- [6] Dieter Vollhardt, Peter Wölfe, *The superfluid phases of Helium 3*, Taylor and Francis, London, 1990.
- [7] Yan Li, Xiaobo Lu, Chunfeng Hou, Double sine-Gordon solitons in nematic liquid crystals under applied electric and magnetic fields, *Journ. of Mod. Opt.* 65, 2006 (2018).
- [8] Y. Tanaka, H. Yamamori, T. Yanagisawa, T. Nishio, S. Arisawa, Experimental formation of a fractional vortex in a superconducting bi-layer, *Physica C* 548, 44 (2018).
- [9] Takashi Yanagisawa, Izumi Hase and Yasumoto Tanaka, Massless and quantized modes of kinks in the phase space of superconducting gaps, *Phys. Lett. A* 382 (2018) 3483.
- [10] Tadashi Uchiyama, Extended hadron model based on the modified sine-Gordon equation, *Phys. Rev. D* 14, 3520 (1976).
- [11] Harold Blas, Exotic baryons in two-dimensional QCD and the generalized sine-Gordon solitons, *JHEP* 03 (2007) 055.
- [12] Harold Blas and Hector L. Carrion, Solitons, kinks and extended hadron model based on the generalized sine-Gordon theory, *JHEP* 01 (2007) 027.
- [13] Vilenkin A, Shellard EPS. *Cosmic strings and other topological defects*. Cambridge U.K.: Cambridge University Press; 1994.
- [14] J. Khoury, B.A. Ovrut, P.J. Steinhardt, N. Turok, *The ekpyrotic universe: colliding branes*

- and the origin of the hot big bang, *Phys. Rev. D* 64 (2001) 123522.
- [15] Mollenauer LF, Gordon JP. Solitons in optical fibers -fundamentals and applications. Burlington: Academic Press; 2006.
- [16] Schneider T. Nonlinear optics in telecommunications. Heidelberg: Springer; 2004.
- [17] Agrawal GP. Nonlinear fiber optics. San Diego: Academic Press; 1995.
- [18] Yakushevich LV. Nonlinear physics of DNA. Weinheim: Wiley-VCH; 2004.
- [19] J. Cuevas-Maraver, P.G. Kevrekidis, F. Williams, *The sine-Gordon Model and Its Applications*, Springer, Heidelberg, 2014.
- [20] Sugiyama, Kink-antikink collisions in the two-dimensional ϕ^4 model, *Prog. Theor. Phys.* 61 (1979) 1550.
- [21] M. Moshir, Soliton-antisoliton scattering and capture in ϕ^4 theory, *Nucl. Phys. B* 185 (1981) 318.
- [22] D.K. Campbell, J.S. Schonfeld, C.A. Wingate, Resonance structure in kink-antikink interactions in ϕ^4 theory, *Physica D* 9 (1983) 1.
- [23] C.A. Wingate, Numerical search for a ϕ^4 breather mode, *SIAM J. Appl. Math.* 43 (1) (1983) 120-140.
- [24] D.K. Campbell, Solitary wave collisions revisited, *Physica D* 18 (1986) 47.
- [25] T.I. Belova, A.E. Kudryavtsev, Quasi-periodic orbits in the scalar classical ϕ^4 field theory, *Physica D* 32 (1988) 18.
- [26] P. Anninos, S. Oliveira, R.A. Matzner, Fractal structure in the scalar $\lambda(\phi^2 - 1)^2$ theory, *Phys. Rev. D* 44 (1991) 1147.
- [27] R.H. Goodman, R. Haberman, Kink-antikink collisions in the ϕ^4 equation: the n-bounce resonance and the separatrix map, *SIAM J. Appl. Dyn. Syst.* 4 (2005) 1195.
- [28] Dorey P., Mersh K., Romanczukiewicz T. and Shnir Y., Kink-antikink collisions in the ϕ^6 model, *Phys. Rev. Lett.* 107 091602 (2011).
- [29] Gani V A, Kudryavtsev A. E., Lizunova M. A., Kink interactions in the (1+1)-dimensional ϕ^6 model, *Phys. Rev. D* 89 125009 (2014).
- [30] Peyrard M., Campbell D. K., Kink-antikink interactions in a modified sine-Gordon model, *Physica D* 9 33-51 (1983).
- [31] Belendryasova E., Gani V., Scattering of the ϕ^8 kinks with power-law asymptotics, *Commun. Nonlinear Sci. Numer. Simul.* 67 414-26 (2019).

- [32] Bazeia D., Belendryasova E., Gani V. A., Scattering of kinks of the sinh-deformed ϕ^4 model, Eur. Phys. J. C 78 340 (2018).
- [33] Simas F. C., Gomes A. R., Nobrega K. Z., Oliveira J. C. R. E., Suppression of two-bounce windows in kink-antikink collisions, J. High Energy Phys. 09 (2016) 104.
- [34] Campbell D. K., Peyrard M., Sodano P., Kink-antikink interactions in the double sine-Gordon equation, Physica D 19 165-205 (1986).
- [35] Haobo Yan, Yuan Zhong, Yu-Xiao Liu, Kei-ichi Maeda, Kink-antikink collision in a Lorentz-violating ϕ^4 model, Phys. Lett. B 807 (2020) 135542.
- [36] A. Alonso Izquierdo, J. Queiroga-Nunes, L. M. Nieto, Scattering between wobbling kinks, Phys. Rev. D 103, 045003 (2021).
- [37] A. R. Gomes, R. Menezes, K. Z. Nobrega, F. C. Simas, Kink-antikink collisions for twin models, Phys. Rev. D 90 (2014) 065022.
- [38] F. C. de Simas, A. R. Gomes, K. Z. Nobrega, Degenerate vacua to vacuumless model and kink-antikink collisions. Phys. Lett. B 775, 290-296 (2017).
- [39] T. S. Mendonça, H. P. de Oliveira, The collision of two-kinks defects, J. High Energy Phys. 09 (2015) 120.
- [40] T. S. Mendonça, H. P. de Oliveira, A note about a new class of two-kinks, J. High Energy Phys. 06 (2015) 133.
- [41] D. Bazeia, A. R. Gomes, K. Z. Nobrega, F. C. Simas, Kink scattering in hyperbolic models, Int. J. Mod. Phys. A 34 (2019) 1950200.
- [42] Fei Z., Kivshar Y., Vazquez L., Resonant kink-impurity interactions in the sine-Gordon model, Phys. Rev. A 45 6019-30 (1992).
- [43] Fei Z., Kivshar Y. S., Vazquez L., Resonant kink-impurity interactions in the ϕ^4 model, Phys. Rev. A 46 5214-20 (1992).
- [44] Malomed B. A., Dynamics and kinetics of solitons in the driven damped double sine-Gordon equation, Phys. Lett. A 136 395 (1989).
- [45] Malomed B. A., Perturbative analysis of the interaction of a ϕ^4 kink with inhomogeneities, J. Phys. A: Math. Gen. 25 755 (1992).
- [46] Goodman R. H., Haberman R., Interaction of sine- Gordon kinks with defects: the two-bounce resonance, Physica D 195 303-23 (2004).
- [47] João G. F. Campos, Azadeh Mohammadi, Fermion transfer in the ϕ^4 model with a half-BPS

- preserving impurity, *Phys. Rev. D* 102, 045003 (2020).
- [48] C. Adam, K. Oles, T. Romanczukiewicz, A. Wereszczynski, Spectral Walls in Soliton Collisions, *Phys. Rev. Lett.* 122 (24) (2019) 241601.
- [49] Javidan K., Interaction of topological solitons with defects: using a nontrivial metric, *J. Phys. A: Math. Gen.* 39 10565 (2006).
- [50] P. Dorey, A. Halavanau, J. Mercer, T. Romanczukiewicz, Y. Shnir, Boundary scattering in the ϕ^4 model, *J. High Energy Phys.* 1705 (2017) 107.
- [51] Fred C. Lima, Fabiano C. Simas, K. Z. Nobrega, Adalto R. Gomes, Boundary scattering in the ϕ^6 model, *J. High Energy Phys.* 10 (2019) 147.
- [52] A.M.Marjaneh, V.A.Gani, D.Saadatmand, S.V.Dmitriev, K.Javidan, Multi-kinkcollisions in the ϕ^6 model. *J. High Energy Phys.* 2017(7), 28 (2017).
- [53] A. M. Marjaneh, D. Saadatmand, K. Zhou, S. V. Dmitriev, M. E. Zomorrodian, High energy density in the collision of n kinks in the ϕ^4 model. *Commun. Nonlinear Sci. Numer. Simul.* 49, 30-38 (2017).
- [54] Patrick Dorey, Tomasz Romanczukiewicz, Resonant kink-antikink scattering through quasinormal modes, *Phys. Lett. B* 779 (2018) 117-123.
- [55] João G. F. Campos, Azadeh Mohammadi, Quasinormal modes in kink excitations and kink-antikink interactions: a toy model, *Eur. Phys. J. C* (2020) 80:352.
- [56] C. Adam, K. Oles, T. Romanczukiewicz, A. Wereszczynski, Kink-antikink scattering in the ϕ^4 model without static intersoliton forces, *Phys. Rev. D* 101, 105021 (2020).
- [57] C. Adam, K. Oles, T. Romanczukiewicz, A. Wereszczynski, Kink-antikink collisions in a weakly interacting ϕ^4 model, *Phys. Rev. E* 102, 062214 (2020).
- [58] J.Y. Huang, S. Chen, Z. Q. Wang, K. Kempa, Y. M. Wang, S. H. Jo, G. Chen, M. S. Dresselhaus, Z. F. Ren, Superplastic carbon nanotubes, *Nature (London)* 439, 281 (2006).
- [59] J.Y. Huang, S. Chen, Z. F. Ren, Z. Q. Wang, D. Z. Wang, M. Vaziri, Z. Suo, G. Chen, and M. S. Dresselhaus, Kink Formation and Motion in Carbon Nanotubes at High Temperatures, *Phys. Rev. Lett.* 97, 075501 (2006).
- [60] X. Y. Li, K. W. Zhang, X. Y. Peng, S. M. Li, X. J. Tan, and J. X. Zhong, Dynamical behavior of the kink motion in carbon nanotubes, *Eur. Phys. J. B* (2012) 85: 64.
- [61] Kévin J. A. Franke, Colin Ophus, Andreas K. Schmid, and Christopher H. Marrows, Switching between Magnetic Bloch and Neel Domain Walls with Anisotropy Modulations, *Phys. Rev.*

- Lett. 127, 127203 (2021).
- [62] F. Martin-Vergara, F. Rus, F. R. Villatoro, Fractal structure of the soliton scattering for the graphene superlattice equation, *Chaos, Solitons & Fractals* 151: 111281 (2021)
- [63] M. Cadoni, R. De Leo, G. Gaeta, A composite model for DNA torsion dynamics, *Phys. Rev. E* 75 (2007) 021919.
- [64] D. Bazeia, V. B. P. Leite, B. H. B. Lima, F. Moraes, Soliton model for proton conductivity in Langmuir films, *Chem. Phys. Lett.* 340 (2001) 205.
- [65] A. Alonso-Izquierdo, Asymmetric kink scattering in a two-component scalar field theory model, *Commun Nonlinear Sci Numer Simulat* 75 (2019) 200-219.
- [66] A. Alonso-Izquierdo, Kink dynamics in a system of two coupled scalar fields in two space-time dimensions, *Physica D: Nonlinear Phenomena* 365, 12-26 (2018).
- [67] A. Alonso-Izquierdo, Kink dynamics in the MSTB model, *Phys. Scr.* 94 (2019) 085302.
- [68] A. Alonso-Izquierdo, Non-topological kink scattering in a two-component scalar field theory model, *Commun Nonlinear Sci Numer Simulat* 85 (2020) 105251.
- [69] A. Alonso-Izquierdo, Reflection, transmutation, annihilation, and resonance in two-component kink collisions, *Phys. Rev. D* 97, 045016 (2018).
- [70] A. Halavanau, T. Romanczukiewicz, Ya. Shnir, Resonance structures in coupled two-component ϕ^4 model, *Phys. Rev. D* 86, 085027 (2012).
- [71] D. Bazeia, M. dos Santos, R. Ribeiro, Solitons in systems of coupled scalar fields, *Physics Letters A* 208 (1) (1995) 84-88.
- [72] A. Hubert and R. Schäfer, *Magnetic domains: the analysis of magnetic microstructures* (Springer, 1998).
- [73] F. A. Brito, F. F. Cruz, J. F. N. Oliveira, Accelerating universes driven by bulk particles, *Phys. Rev. D* 71, 083516 (2005).
- [74] D. Bazeia, W. Freire, L. Losano, R.F. Ribeiro, Topological defects and the trial orbit method, *Mod. Phys. Lett. A* 17 (2002) 1945.
- [75] A. Alonso Izquierdo, M.A. Gonzalez Leon, and J. Mateos Guilarte, Kink variety in systems of two coupled scalar fields in two space-time dimensions, *Phys. Rev. D* 65, 085012 (2002).
- [76] D. Bazeia, J. R. S. Nascimento, R. F. Ribeiro, D. Toledo, Soliton stability in systems of two real scalar fields, *J. Phys. A: Math. Gen.* 30 (1997) 8157-8166.
- [77] D. Bazeia, Henrique Boschi-Filho, Francisco A. Brito, Domain defects in systems of two real

scalar fields, JHEP 04 (1999) 028.

- [78] Hans-Benjamin Braun, Fluctuations and instabilities of ferromagnetic domain-wall pairs in an external magnetic field, Phys. Rev. B 50, 16485 (1994).